



Short communication

Changes in the properties and structure of hydrogen-storage electrodes after long-term charge/discharge cycling

Zhen Zhou, Jie Yan^{*}, Yuxuan Li, Deying Song, Yunshi Zhang*Institute of New Energy Material Chemistry, Nankai University, Tianjin 300071, China*

Received 1 August 1997; accepted 25 August 1997

Abstract

Studies are focused on the changes in the properties and structure of hydrogen-storage alloy electrodes used in Ni/MH batteries after long-term cycling. Experimental results show that the alloys are pulverized after a large number of cycles and $\text{La}(\text{OH})_3$, $\text{Al}(\text{OH})_3$ and LiMnO_2 are formed on the surface of the alloy. This results in degradation of the hydrogen-storage alloy electrodes. © 1998 Elsevier Science S.A.

Keywords: Hydrogen-storage electrodes; Charge/discharge cycling; Ni/MH batteries

1. Introduction

The Ni/MH battery has been developed as a replacement for the Ni/Cd battery. The Ni/MH battery has higher specific energy and almost the same voltage as the conventional Ni/Cd battery [1]. Also, it offers better overall performance in terms of higher rate capacity, good low-temperature dischargeability, no memory effects, and long cycle life [2–7].

The properties of Ni/MH batteries are dependent upon the qualities of the positive and negative electrodes. In particular, the hydrogen-storage alloys which are utilized in the negative electrodes tend to be oxidized and pulverized such that the ability of absorbing and desorbing hydrogen is lost. Thus, many surface modification methods have been developed to improve the performance of the negative electrode [8]. Willems and Buschow [9] have studied the degradation process of LaNi_5 -based alloy electrodes in a so-called electrochemical half-cell, and have found that the capacity decay upon charge–discharge cycling is due to the decomposition and oxidation of the alloys to form $\text{La}(\text{OH})_3$.

In this investigation, some experimental Ni/MH batteries (AAA size, 400 mA h capacity) are prepared using $\text{LmNi}_{3.8}\text{Co}_{0.5}\text{Mn}_{0.4}\text{Al}_{0.2}\text{Li}_{0.1}$ (where Lm denotes lanthanum-rich Mischmetal) alloy [10] coated with nickel as

the negative material and spherical $\text{Ni}(\text{OH})_2$ as the positive material. Continuous charge–discharge experiments are carried out at the 1 C rate. When the discharge capacity decay reaches 30%, the properties and structure of the negative electrode alloy are examined.

2. Experimental

$\text{LmNi}_{3.8}\text{Co}_{0.5}\text{Mn}_{0.4}\text{Al}_{0.2}\text{Li}_{0.1}$ alloy coated with nickel was used as the negative electrode material and spherical $\text{Ni}(\text{OH})_2$ as the positive electrode material. After mixing, respectively, with conductive substances such as Ni or Co powder and binders such as PVA and PTFE dispersions, materials were incorporated in nickel foams (those of positive electrodes were spot-welded to nickel ribbon current-collectors) with a spatula. The electrodes were dried in air at room temperature and then pressed.

A separator was inserted between the electrodes, which were then rolled and inserted into AAA-type battery cans. A 6 M KOH–15 g/l LiOH aqueous solution was injected. Finally, the batteries were sealed.

The batteries were activated by charge–discharge cycling at a low rate, and were then subjected to cycle-life testing. Charging was carried out to 150% of positive electrode capacity at the 1 C rate, and after a 30-min rest, discharging was performed to 1 V at the 1 C rate. All the tests were conducted at room temperature, and when the capacity decay reached 30%, the tests were stopped.

^{*} Corresponding author.

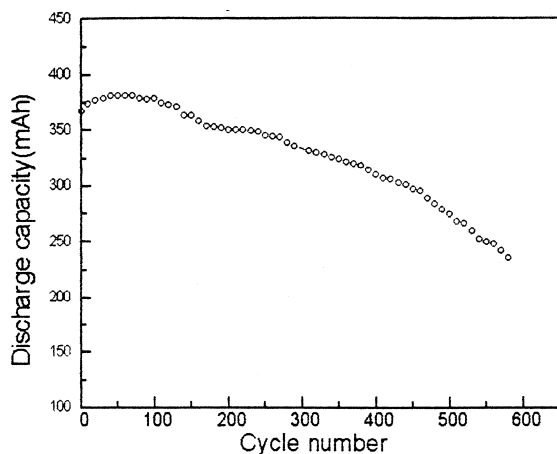


Fig. 1. Variation in discharge capacity with cycle number for experimental Ni/MH battery (charge and discharge rate: 1 C).

After cycling, the batteries were cut open, and immersed in alkaline solution. Then the discharge curves (charge at 0.1 C rate, discharge at 0.2 C rate) of the alloys before and after cycling were recorded at room temperature using sintered Ni(OH)_2 counter electrodes and a Hg/HgO/6 M KOH reference electrode.

The surface morphology of the alloys was analyzed by scanning electron microscopy (SEM). The structure, before and after cycling, was analyzed by X-ray diffraction (XRD).

3. Results and discussion

3.1. Cycle life

The discharge capacity and average voltages in each cycle of an experimental Ni/MH battery were measured at room temperature and are shown in Figs. 1 and 2, respectively. During the first 100 cycles, there is an increase in

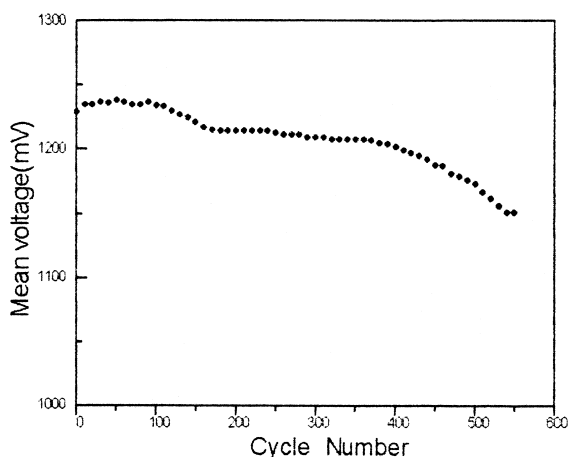


Fig. 2. Variation in average voltage with cycle number for experimental Ni/MH battery (charge and discharge rate: 1 C).

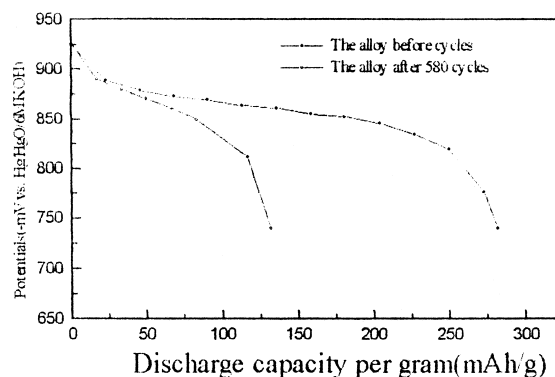


Fig. 3. Discharge curves for alloy electrodes before and after cycles (charge rate: 0.1 C; discharge rate: 0.2 C).

both the capacity and the voltage. This suggests that the battery is still undergoing activation. After 100 cycles, the two parameters began to decrease. The decay in capacity was 30% after 580 cycles.

3.2. Electrochemical tests

The capacity of the alloy electrode on immersion in an excess of alkaline solution after 580 cycles is much lower than that of the alloy electrode before cycling (see Fig. 3). This indicates that the capacity decay of the Ni/MH battery is caused, not only by a deficiency in electrolyte during a large number of cycles, but also by degradation of the electrodes.

3.3. Morphology and structure

Electron micrographs of the alloys before and after cycling are presented in Fig. 4a. The alloy particles before cycling have a smooth surface and a large size, but after 580 cycles the alloy is pulverized and porous. There is line broadening of the peaks in the XRD spectra on cycling (see Fig. 5). This also proves that the alloy has become pulverized. It is also found from the spectra that the alloy both before and after cycling has predominantly a CaCu_5 -

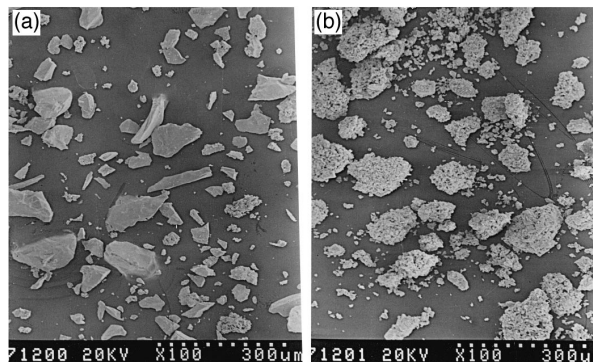


Fig. 4. Electron macrographs $\times 8000$ for the alloy: (a) before cycling and (b) after 580 cycles.

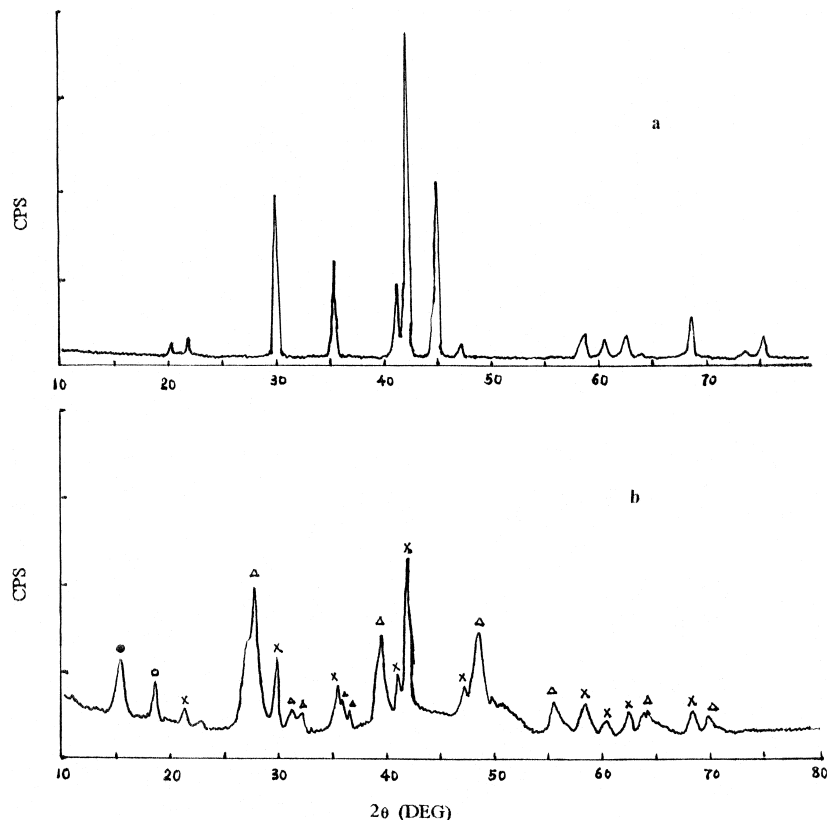


Fig. 5. X-ray diffraction spectra for the alloy: (a) before cycling; (g) after 580 cycles (b). (●, LiMnO_2 ; ○, Al(OH)_3 ; △, La(OH)_3 ; ×, $\text{LmNi}_{3.8}\text{Co}_{0.5}\text{Mn}_{0.4}\text{Al}_{0.2}\text{Li}_{0.1}$).

type structure. Nevertheless, the XRD peaks of the alloy are weakened after 580 cycles, and this indicates that part of the alloy has been destroyed. Furthermore, diffraction peaks for La(OH)_3 , Al(OH)_3 and LiMnO_2 appear and signify that these substances are formed on the surface of the alloy after an extensive cycling. Willems and Buschow [9] have studied the degradation process of LaNi_5 -based alloys and have shown that the formation of La(OH)_3 inhibits hydrogen absorption. As for the formation of Al(OH)_3 , the same authors have pointed out that, unless the volume expansion is too large, the Al(OH)_3 layer surrounding the alloy particles has a protective effect against the electrolyte. Manganese substitutions for nickel are known to lower the plateau pressure, but also lower the cycling stability [11]. The alloy used in the experiments reported here contains a small amount of lithium (15 g/l LiOH was added to 6 M KOH solution) and LiOH also participates in the corrosion to the alloy. Thus, the formation of LiMnO_2 is observed.

4. Conclusions

The $\text{LmNi}_{3.8}\text{Co}_{0.5}\text{Mn}_{0.4}\text{Al}_{0.2}\text{Li}_{0.1}$ alloy used as a negative electrode for Ni/MH batteries tends to be pulverized, and oxidized to form La(OH)_3 , Al(OH)_3 and LiMnO_2 are

formed during long-term cycling and accordingly, the discharge capacity and average voltage of the Ni/MH battery decrease gradually. In order to improve further the performance of Ni/MH batteries, studies should be focused on how to minimize to oxidation and pulverization of the negative electrode alloys.

References

- [1] T. Sakai, H. Yoshinaga, H. Miyamura, N. Kuriyama, H. Ishikawa, J. Alloys Comp. 180 (1992) 37.
- [2] A. Anani, A. Visintin, K. Petrov, S. Srinivasan, J. Power Sources 47 (1994) 261.
- [3] K. Suzuki, N. Yanagihara, K. Kawano, A. Dhta, J. Alloys Comp. 192 (1993) 173.
- [4] A.H. Boonstra, T.N.M. ernards, J. Less-Common Met. 159 (1990) 327.
- [5] M. Geng, D.O. Northwood, Int. J. Hydrogen Energy 21 (1996) 887.
- [6] J.-H. Lee, K.-Y. Lee, S.-M. Lee, J.-Y. Lee, J. Alloys Comp. 221 (1995) 174.
- [7] Y.-Q. Lei, Z.-P. Li, C.-P. Chen, J. Wu, Q.-D. Wang, J. Less-Common Met. 172–174 (1991) 1265.
- [8] C. Iwakura, M. Matsuoka, K. Asai, T. Kohnno, J. Power Sources 38 (1992) 335.
- [9] J.J.G. Willems, K.P.H.J. Buschow, J. Less-Common Met. 129 (1987) 13.
- [10] Y. Zhang, D. Song, US Pat. 5,242,656 (1993).
- [11] F. Meli, A. Zuttel, L. Schlapbach, J. Alloys Comp. 202 (1993) 8.